Measurement of hard double-partonic interactions in W $\rightarrow$ lν + 2 jet events using the ATLAS detector at the LHC

Eleanor Dobson for the ATLAS Collaboration

DOI: http://dx.doi.org/10.3204/DESY-PROC-2012-03/15

The production of W bosons in association with two jets has been investigated using proton-proton collisions at a centre-of-mass energy of $\sqrt{s} = 7$ TeV. The fraction of $W+2$ jet events arising from double parton scattering was measured to be $f_{\rm DP}^{\rm R} = 0.16 \pm 0.01$ (stat) $\pm$ 0.03 (sys) for jets with transverse momentum $p_{\rm T} > 20$ GeV and rapidity $|y| < 2.8$. This corresponds to an effective cross section for hard double partonic interactions of $\sigma_{\rm eff} = 11 \pm 1$ (stat) $^{+3}_{-2}$ (sys) mb, which is consistent with previous measurements performed at lower centre-of-mass energies in different channels. This measurement was performed using data collected with the ATLAS detector corresponding to an integrated luminosity of 33 pb^{-1} .

1 Principle of the measurement

The aim of this analysis, described in detail in [1], is to extract the fraction of $W + 2$j events[1] containing hard double parton interactions (DPI) produced in proton-proton collisions recorded by the ATLAS detector. The method of extraction is to fit over the distribution of a variable that has good discrimination between a W boson produced in direct association with 2 jets ($W + 2{\rm j}_{\rm D}$) and a W boson produced in association with zero jets in addition to a double-parton scatter resulting in two jets ($W_0 + 2{\rm j}_{\rm DPI}$).

The fraction of $W_0 + 2{\rm j}_{\rm DPI}$ events in the selected $W + 2$j sample at reconstruction level R, $f_{\rm DP}^{\rm R}$, is defined as

$$f_{\rm DP}^{\rm R} = \frac{N_{W_0+2{\rm j}_{\rm DPI}}}{N_{W+2{\rm j}}}, \tag{1}$$

where $N_{W_0+2{\rm j}_{\rm DPI}}$ is the number of $W_0+2{\rm j}_{\rm DPI}$ events passing $W+2$j selection, and $N_{W+2{\rm j}}$ is the total number of events passing $W + 2$j selection. Although these quantities will be measured at detector level, it is shown in Section 5.3 that $f_{\rm DP}^{\rm R}$ is closely related to its parton-level (P) equivalent, $f_{\rm DP}^{\rm P}$. It is possible to define the effective cross section [2] $\sigma_{\rm eff}$

$$\sigma_{\rm eff} = \frac{\sigma_{W_0} \cdot \sigma_{2{\rm j}}}{\sigma_{W_0+2{\rm j}_{\rm DPI}}}, \tag{2}$$

where σ_{W_0}, $\sigma_{W_0+2{\rm j}_{\rm DPI}}$ and $\sigma_{2{\rm j}}$ are the cross-sections of $W+0$j, $W_0+2{\rm j}_{\rm DPI}$ and dijet (2j) events

[1] $W + {\rm n j}$ will be used to denote processes in which W is produced in association with n-jets

respectively. Each cross-section can be calculated using

$$\sigma = \frac{N}{A\ \epsilon\ \mathscr{L}}, \tag{3}$$

where N is the number of events, A is the acceptance after reconstruction and unfolding corrections, ϵ is the trigger efficiency and $\mathscr{L}$ is the integrated luminosity. Equation (2) can therefore be rewritten as

$$\sigma_{\text{eff}} = \frac{1}{f_{\text{DP}}^{\text{R}}} \cdot \frac{N_{W_0}\ N_{2\text{j}}}{N_{W+2\text{j}}} \cdot \frac{A_{W_0+2\text{j}_{\text{DPI}}}}{A_{W_0}\ A_{2\text{j}}} \cdot \frac{\epsilon_{W_0+2\text{j}_{\text{DPI}}}}{\epsilon_{W_0}\ \epsilon_{2\text{j}}} \cdot \frac{\mathscr{L}_{W_0+2\text{j}_{\text{DPI}}}}{\mathscr{L}_{W_0}\ \mathscr{L}_{2\text{j}}}. \tag{4}$$

In this analysis, a factorisation ansatz between the W and the 2j systems is assumed. This leads to a number of conclusions regarding the quantities in equation (4). First, the kinematics of the W do not influence the kinematic distributions of the DPI system. This implies that

$$A_{W_0+2\text{j}_{\text{DPI}}} = A_{W_0} \cdot A_{2\text{j}_{\text{DPI}}}, \tag{5}$$

once corrections involving the impact of jets on W reconstruction and vice versa have been made (discussed in detail in Section 5.4). Secondly, the kinematics of the jets in the DPI system may be modelled by the kinematics of single-scatter dijet events, which implies that

$$A_{2\text{j}_{\text{DPI}}} = A_{2\text{j}}. \tag{6}$$

Finally, the $W_0 + 2\text{j}_{\text{DPI}}$ and W_0 events will be selected online using the same trigger selection. This results in luminosity and efficiency cancellations and equation (4) simplifies to

$$\sigma_{\text{eff}} = \frac{1}{f_{\text{DP}}^{\text{R}}} \cdot \frac{N_{W_0}\ N_{2\text{j}}}{N_{W+2\text{j}}} \cdot \frac{1}{\epsilon_{2\text{j}}} \cdot \frac{1}{\mathscr{L}_{2\text{j}}}. \tag{7}$$

In this analysis the terms in equation (7) are determined as separate quantities allowing the evaluation of σ_{eff} with its associated uncertainty.

2 Event selection

The measurement was performed using 33 $\text{pb}^{-1}$of data taken with the ATLAS detector [3] during 2010. Events were required to contain at least one primary vertex that was reconstructed within 200 mm of the interaction point and contained at least three tracks. Additional cuts were applied to reduce the contamination from noisy calorimeter cells, beam backgrounds and cosmic rays.

The selection of the $W \to \ell\nu$ signal was similar to that used in the $W \to \ell\nu$ + jets cross-section analysis [4]. Dedicated single-electron and single-muon trigger selections were used to retain $W \to e\nu$ and $W \to \mu\nu$ events, respectively.

In the electron channel, events were required to contain one electron that satisfied tight identification criteria with transverse momentum $p_{\text{T}} > 20$ GeV and pseudorapidity $|\eta| < 2.47$. Electrons reconstructed in the transition region between the barrel and endcap calorimeters ($1.37 < |\eta| < 1.52$) were excluded from the analysis. Additional requirements were applied to remove electrons falling into inactive regions of the calorimeter.

In the muon channel, events were required to contain an isolated, prompt muon with $p_{\text{T}} > 20$ GeV and pseudorapidity $|\eta| < 2.5$. The muon was reconstructed from information from both the muon spectrometer and the inner detector.

In both channels, additional requirements were placed on $E_{\mathrm{T}}^{\mathrm{miss}}$ and transverse mass M_{T}. Events were required to have transverse missing energy $E_{\mathrm{T}}^{\mathrm{miss}} > 25$ GeV and $M_{\mathrm{T}} > 40$ GeV.

Jets are defined using the anti-k_t [5] algorithm with $R = 0.6$ and full four momentum recombination. The jets are reconstructed from electromagnetic scale topological clusters that are built from calorimeter cells. Each jet is subsequently corrected using p_{T} and η dependent jet energy scale (JES) calibration factors derived from simulated Monte Carlo (MC) events [6]. Jets were required to have $p_{\mathrm{T}} > 20$ GeV and $|y| < 2.8$. All jets within $\Delta R < 0.5$ of a reconstructed electron or muon were removed from the analysis. Jets originating from pile-up interactions were removed by applying a cut on the jet-vertex fraction (JVF), which was defined for each jet in the event.

Events were subsequently divided into two orthogonal datasets. The first was a $W + 0$j sample, in which no jets were reconstructed – in accordance with the definition above – in addition to the W decay products. The second was the $W + 2$j sample, in which exactly two additional jets were reconstructed. The $W + 0$j sample is only used for the evaluation of σ_{eff}.

Dijet events were selected online using a trigger selection derived from the Minimum Bias Trigger Scintillators and Zero Degree Calorimeters, which have been shown to be unbiased and fully efficient for jet-based measurements [6]. Dijet events were required to contain exactly two jets, reconstructed using the same algorithm, input objects and kinematic selection as in the previous section.

3 Monte Carlo simulation

Alpgen [7] was used to generate $W + n$j signal events. MLM [8] matching was used, with the matching scale cut set at 20 GeV, to prevent any double counting caused by the parton shower. Alpgen is a matrix element generator that is interfaced to Herwig [9] v6.510, for parton showering and hadronisation, and to Jimmy [10] v4.31, for the underlying event. The event generator tune was AUET1 [11]. Sherpa [12] v1.3.1 was also used to generate an alternative sample of $W + n$j signal events. Sherpa is a matrix element generator that uses CKKW [13] matching to prevent double counting from the parton shower. The Sherpa samples were generated with the default underlying event tune and the CKKW matching cut at 30 GeV. As a final comparison for signal events, Pythia6 [14] was used to generate inclusive W events, with the AMBT1 tune [15] for the underlying event activity.

Various generators were used to simulate the effect of physics backgrounds to the W signal events. $t\bar{t}$ events were generated at next-to-leading order accuracy using the MC@NLO [16] generator. MC@NLO was interfaced to Herwig and Jimmy, and the AUET1 tune for the underlying event was used in the sample generation. Backgrounds from dijet and inclusive Z production were simulated using Pythia6 with tune AMBT1 for the underlying event.

Each generated event was passed through the standard ATLAS detector simulation [17], which is based on Geant4 [18]. The MC events were reconstructed and analysed using the same chain as applied to the data.

3.1 Event generator samples without double parton scattering

In addition to the standard MC simulation, $W + 2$j events with no multiple parton interactions were generated using Sherpa and Alpgen+Herwig+Jimmy. These samples model the jet-jet correlations in the non-DPI production of $W + 2$j events and were used to extract $f_{\mathrm{DP}}^{\mathrm{R}}$

from the data. DPI was switched off in Sherpa using the `MI_HANDLER` switch. This prevents secondary parton-parton scattering with $p_{\mathrm{T}} \gtrsim 5$ GeV. The initial/final state radiation from the incoming/outgoing legs of the leading-order matrix element is retained, in addition to the generation of intrinsic transverse momentum and fragmentation of beam remnants.

To create a corresponding Alpgen+Herwig+Jimmy sample with DPI switched off, the standard generation of $W+2$j was used, but events were rejected if the two jets were identified as originating from a non-primary parton-parton scatter. This jet-parton matching was performed using the Herwig event record, by identifying the parton with status code 123/124 and $p_{\mathrm{T}} > 3.5$ GeV that was closest to each jet[2].

4 Characteristics of DPI events in data and MC

The goal of this study is to identify the fraction of $W + 2$j events that are produced via double parton scattering. It is expected that the two partonic scatters are independent and therefore the jets produced in DPI events will typically be produced more back-to-back in azimuth than those produced in single scatter events. The independence of the two scatters can also be seen in variables that parameterise the transverse momentum imbalance between the jets, such as

$$\Delta_{\mathrm{jets}} = \left|\vec{p}_{\mathrm{T},1} + \vec{p}_{\mathrm{T},2}\right| \qquad \text{and} \qquad \Delta^{\mathrm{n}}_{\mathrm{jets}} = \frac{\left|\vec{p}_{\mathrm{T},1} + \vec{p}_{\mathrm{T},2}\right|}{\left|\vec{p}_{\mathrm{T},2}\right| + \left|\vec{p}_{\mathrm{T},2}\right|}, \tag{8}$$

where the indices 1 and 2 identify the two jets in the event.

The Sherpa and Alpgen+Herwig+Jimmy predictions for Δ_{jets} are shown in Figure 1[3], with and without the contribution from double parton scattering. The effect of including the DPI in each generator is an enhancement in the region $\Delta_{\mathrm{jets}} \sim 10$ GeV. It is concluded that this enhancement is related to the DPI contribution, for which the two jets are produced back-to-back in azimuth and with similar transverse momenta. The distribution of the $\Delta^{\mathrm{n}}_{\mathrm{jets}}$ variable is also shown in Figure 1. This variable is constructed such that the region close to $\Delta^{\mathrm{n}}_{\mathrm{jets}}$=1 contains no DPI, and that near $\Delta^{\mathrm{n}}_{\mathrm{jets}}$=0 contains a larger fraction of DPI. The $\Delta^{\mathrm{n}}_{\mathrm{jets}}$ variable is particularly useful, because, as a ratio, it has reduced sensitivity to jet energy uncertainties whilst remaining sensitive to the presence of DPI.

5 Extraction of $\mathbf{f^{R}_{DP}}$

The extraction of $f^{\mathrm{R}}_{\mathrm{DP}}$ from the data was performed using a χ^2 minimisation to the normalised $\Delta^{\mathrm{n}}_{\mathrm{jets}}$ distribution of the form

$$(1 - f^{\mathrm{R}}_{\mathrm{DP}}) \cdot A + f^{\mathrm{R}}_{\mathrm{DP}} \cdot B, \tag{9}$$

where template A is the normalised distribution for $W + 2\mathrm{j}_{\mathrm{D}}$ and template B is the normalised distribution for $W_0 + 2\mathrm{j}_{\mathrm{DPI}}$. The construction of these templates is discussed in Section 5.1. To minimise the dependence on near-collinear jets, the two bins covering $0.933 < \Delta^{\mathrm{n}}_{\mathrm{jets}} < 1.0$ were not used in the fit.

[2]The threshold was chosen to be 3.5 GeV to approximately match the `PTJIM` parameter (3.86 GeV), which is used in Jimmy to set the transverse momentum scale of secondary scatters.

[3]as for all figures in this note, these have been reproduced from [1].

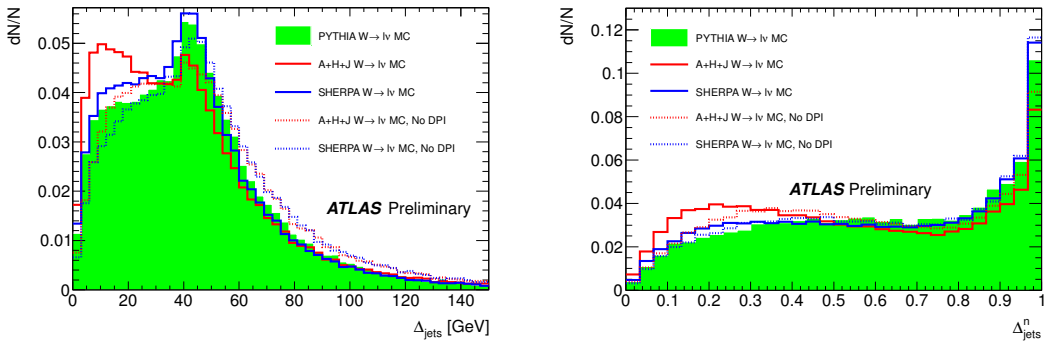

(a) (b)

Figure 1: Predicted distributions of Δ_{jets} (a) and $\Delta^{\text{n}}_{\text{jets}}$ (b) in $W \to \ell\nu$+2 jet events in SHERPA and ALPGEN+HERWIG+JIMMY (A+H+J) Monte Carlo simulation when DPI is switched on and off in the manner described in Section 3. The PYTHIA prediction (with DPI switched on) is also shown for comparison. All distributions are normalised to unity.

5.1 Template construction

The model for the $W + 2\text{j}_{\text{D}}$ contribution (template A) was taken from the event generator predictions. The first model for this template was the SHERPA prediction with the MPI switched off. The second model was the ALPGEN+HERWIG+JIMMY prediction with the MPI removed. The procedure to switch off or remove MPI in the generators was discussed in Section 3. There is a small difference between the SHERPA and ALPGEN+HERWIG+JIMMY predictions, which will be used as a generator modelling uncertainty in the extraction of f^{R}_{DP}. This is discussed further in Section 5.3.

Template B, the model for $W_0 + 2\text{j}_{\text{DPI}}$ kinematics, is constructed from dijet data using the selection outlined in Section 2. The fractional difference between the extracted value of f^{R}_{DP} when using dijet MC in place of dijet data was found to be negligible.

5.2 Fit results

The result of fitting the templates to the data is shown in Figure 2. The fraction of DPI events was found to be $f^{\text{R}}_{\text{DP}} = 0.18$, using the SHERPA prediction for template A. The associated quality of the fit was $\chi^2/N_{\text{df}} = 1.4$ ($N_{\text{df}} = 27$). The fraction of DPI was observed to be $f^{\text{R}}_{\text{DP}} = 0.14$ using the ALPGEN+HERWIG+JIMMY prediction for template A, with a χ^2/N_{df} of 0.9. The final value of f^{R}_{DP} was taken to be the average of these results ($f^{\text{R}}_{\text{DP}} = 0.16$). The statistical uncertainty was obtained by varying the χ^2 by one unit and was found to be $\simeq 0.07 f^{\text{R}}_{\text{DP}}$. The systematic uncertainties on the extracted value of f^{R}_{DP} are discussed in Section 5.4.

The value f^{R}_{DP} extracted from the fit to $\Delta^{\text{n}}_{\text{jets}}$ can be used to normalise appropriate templates for Δ_{jets}. Figure 3 shows the distribution obtained in data compared to these normalised templates.

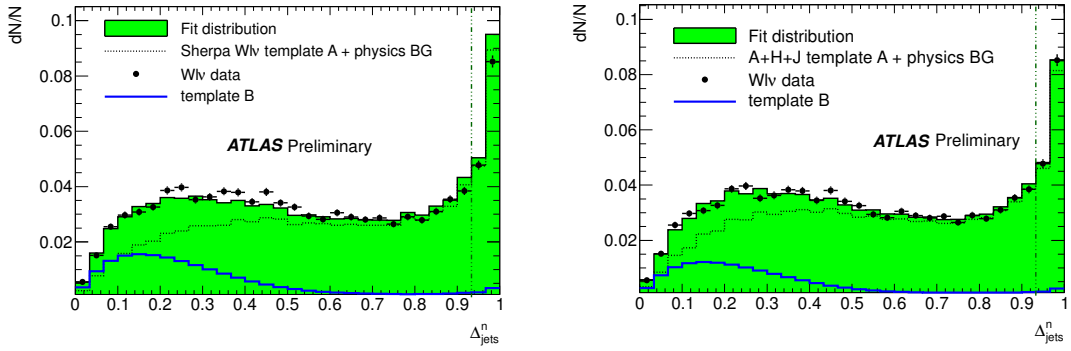

(a) (b)

Figure 2: Comparison of Δ^{n}_{jets} distribution in the data with expectations after χ^2 minimisation fits of the templates to data to extract f^{R}_{DP}. The result obtained using Sherpa for template A is shown in (a) and the result obtained using Alpgen+Herwig+Jimmy (A+H+J) for template A is shown in (b). The physics background (physics BG) is added to template A in the figure (dotted line). The fit region is the region to the left of the dotted line. Data and the overall fit were normalised to unity, template A to $1 - f^{R}_{DP}$ and template B to f^{R}_{DP}.

5.3 Transition of results from detector to parton level

In this section, the relationship between the parton-level, f^{P}_{DP}, and reconstruction level, f^{R}_{DP}, quantities is established. The fraction of events originating from double parton scattering is defined at parton-level by

$$f^{P}_{DP} = \frac{N^{P}_{W_0+2j_{DPI}}}{N^{P}_{W_0+2j_{DPI}} + N^{P}_{W+2j_{D}}}. \tag{10}$$

where $N^{P}_{W_0+2j_{DPI}}$ is the number of events generated with the two partons originating from DPI and $N^{P}_{W+2j_{D}}$ is the number of events generated with the two partons produced directly from the $W + 2j$ matrix element. The partons are required to pass the same selection criteria as the reconstructed jets, $p_T > 20$ GeV and $|y| < 2.8$. The value of f^{P}_{DP} was evaluated to be 0.18 in the nominal Alpgen+Herwig+Jimmy settings.

DPI events were weighted with a factor x to vary this default value of f^{P}_{DP} in the sample. A χ^2 minimisation fit to this weighted sample was then performed, with the SHERPA prediction for template A and the dijet data for template B. The result of the fit yields an estimate of the fraction of DPI present in the detector level Monte Carlo, f^{T}_{DP}.

The result of the fit is shown in Figure 4(a) for $f^{P}_{DP} = 0.18$ ($x = 1$). The relationship between f^{T}_{DP} and f^{P}_{DP} is obtained by varying x and is shown in Figure 4(b). In general, there is a strong correlation between the extracted value of f^{T}_{DP} and the input value of f^{P}_{DP}. There is, however, a small bias of f^{T}_{DP} at small values of f^{P}_{DP}. This bias arises from (i) modelling differences between the two generators and (ii) physics and detector effects present in the transition from parton-level to detector-level. As the fraction of DPI is increased, the fit result becomes increasingly insensitive to the details of template A and the extracted value of f^{T}_{DP} converges towards the input value of f^{P}_{DP}.

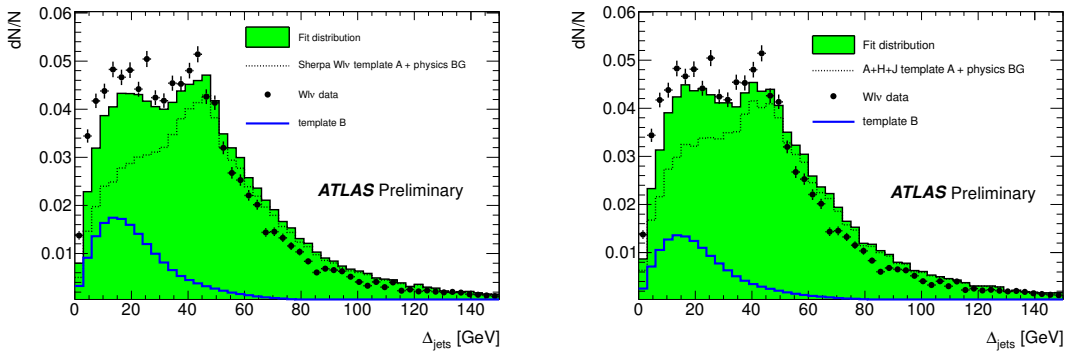

(a) (b)

Figure 3: Comparison of Δ_{jets} distribution in the data with expectations of template A and B combined in the ratio N_B/N_A=f_{DP}^{R}/(1-f_{DP}^{R}), where f_{DP}^{R} is fixed to the value obtained in the fit to the $\Delta_{\text{jets}}^{\text{n}}$ distribution. The prediction using SHERPA for template A is shown in (a) and ALPGEN+HERWIG+JIMMY is shown in (b). The physics background (physics BG) is added to template A in the figure (dotted line). Data and the overall fit were normalised to unity, template A to $1 - f_{\text{DP}}^{\text{R}}$ and template B to f_{DP}^{R}.

5.4 Systematic uncertainty on f_{DP}^{R}

In Section 5.2, the final value of $f_{\text{DP}}^{\text{R}} = 0.16$ was determined using both the SHERPA and the ALPGEN+HERWIG+JIMMY predictions for template A. In particular, the value of f_{DP}^{R} was taken to be the average of the values extracted using the two event generators. The systematic uncertainty associated with the event generator modelling of $W + 2\text{j}_{\text{D}}$ is taken to be the difference between this average and the generator-based predictions. This is the largest systematic uncertainty in the measurement and observed to be $0.12 f_{\text{DP}}^{\text{R}}$. Furthermore, in Section 5.3, the shift between f_{DP}^{P} and f_{DP}^{T} at $f_{\text{DP}}^{\text{T}} = 0.16$ was observed to be $0.1 f_{\text{DP}}^{\text{R}}$. This is taken to represent the systematic uncertainty in the use of reconstructed objects to measure a quantity that is formally defined at the parton-level. It is noted that these estimates partially double count the effects of the modelling differences between SHERPA and ALPGEN+HERWIG+JIMMY.

Events in which $W + 1\text{j}_{\text{D}}$ is produced in conjunction with a DPI scatter were observed to have little impact on the analysis. At parton level, the shift in f_{DP}^{P} was found to be negligible if these events were included. Furthermore, the addition of these events at reconstruction level did not significantly alter the shape of template A. It is therefore concluded that the systematic uncertainty due to such combinatoric events is negligible. The impact of physics modelling was observed to be negligible for the electroweak and $t\bar{t}$ backgrounds. For the QCD background, the normalisation uncertainty derived in [4] was included, resulting in a physics background modelling uncertainty of 1% on f_{DP}^{R}.

The systematic uncertainty on f_{DP}^{R} due to jet energy scale calibration was found to be $0.1 f_{\text{DP}}^{\text{R}}$. The systematic uncertainty due to the jet energy resolution was observed to be negligible. Both of these effects were calculated after varying the jet energy scale and resolution within the known uncertainties [6]. The impact of pileup was obtained by studying the fit results as a function of the number of primary vertices reconstructed in the event. The effect of removing the JVF selection criterion was studied, as an additional estimate of the uncertainty due to pile-up. The

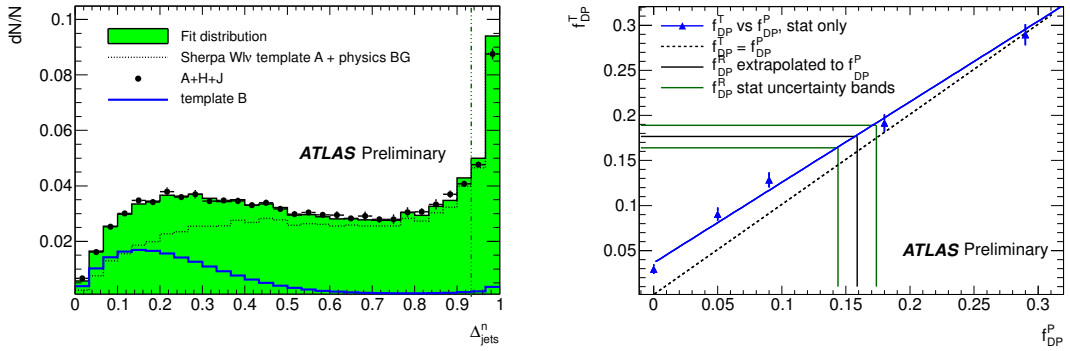

(a) (b)

Figure 4: (a) Comparison of $\Delta^{\mathrm{n}}_{\mathrm{jets}}$ distribution predicted by the Alpgen+Herwig+Jimmy default ($x = 1$) with χ^2 minimisation fits of templates A (Sherpa) and B, to extract $f^{\mathrm{T}}_{\mathrm{DP}}$. The template construction and normalisation is the same as in Figure 2. (b) Extracted value of $f^{\mathrm{T}}_{\mathrm{DP}}$ as a function of $f^{\mathrm{P}}_{\mathrm{DP}}$. A one-to-one correspondence line (dashed line) and a linear fit (unbroken line) to the points are also shown. The data extracted value $f^{\mathrm{R}}_{\mathrm{DP}}$ (using the Sherpa prediction of template A) with its statistical uncertainty of 0.07 $f^{\mathrm{R}}_{\mathrm{DP}}$ is also shown extrapolated to the parton level using the linear fit.

overall systematic uncertainty on $f^{\mathrm{R}}_{\mathrm{DP}}$ due to pileup was estimated to be $0.08 f^{\mathrm{R}}_{\mathrm{DP}}$. The trigger used to select dijet events is 100% efficient in selecting dijet events and so should not bias their observed kinematics [6]. However, an additional uncertainty of 5% was included after studying the variation in the template B shape when the calorimeter jet trigger was used to select the events.

The sources of systematic uncertainty discussed in this section are summed in quadrature to give an overall systematic uncertainty of 21% in the measurement of $f^{\mathrm{R}}_{\mathrm{DP}}$.

5.5 Dependence of $f^{\mathrm{R}}_{\mathrm{DP}}$ on phase space cuts

Figure 5 shows the values of $f^{\mathrm{P}}_{\mathrm{DP}}$, $f^{\mathrm{T}}_{\mathrm{DP}}$ and $f^{\mathrm{R}}_{\mathrm{DP}}$ as a function of the minimum jet p_{T} requirement. The extracted values of $f^{\mathrm{T}}_{\mathrm{DP}}$ and $f^{\mathrm{R}}_{\mathrm{DP}}$ are presented only for phase space regions in which the jet energy scale is well understood and the measurement is statistically feasible. The decrease of $f^{\mathrm{R}}_{\mathrm{DP}}$ with increasing jet p_{T} is consistent with the MC predictions for $f^{\mathrm{P}}_{\mathrm{DP}}$ and $f^{\mathrm{T}}_{\mathrm{DP}}$. This decrease reflects the fact that the partons originating from the additional scatters have a steeper p_{T} distribution than the partons from the primary scatter. The values of $f^{\mathrm{P,T,R}}_{\mathrm{DP}}$ were observed to be only weakly correlated with the maximum rapidity requirement applied to the partons/jets and is not discussed further.

6 Evaluation of σ_{eff}

The value of σ_{eff} was evaluated using equation 7. The fraction of events from double parton scattering was extracted from the data as discussed in the previous section. The exclusivity ratio, $N_{W_0}/N_{W+2\mathrm{j}}$ was obtained using the inclusive W dataset produced with the selection

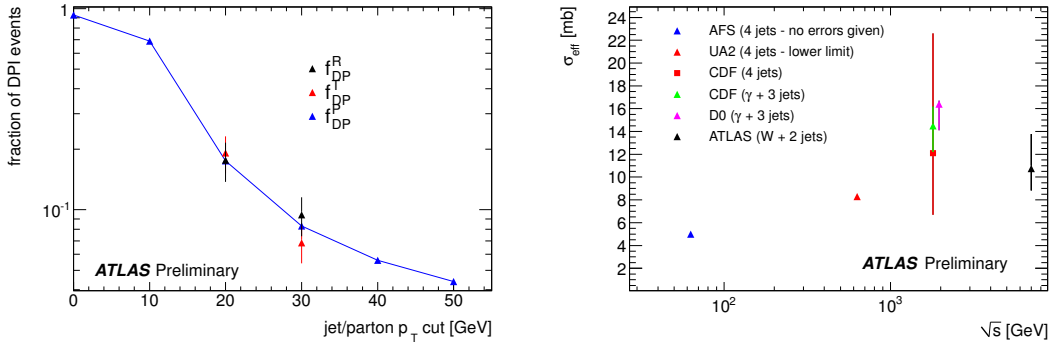

(a) (b)

Figure 5: (a) Extracted values of $f_{\mathrm{DP}}^{\mathrm{T}}$, $f_{\mathrm{DP}}^{\mathrm{P}}$ and $f_{\mathrm{DP}}^{\mathrm{R}}$ (using SHERPA prediction for template A) as a function of jet/parton p_{T}, and (b) the centre-of-mass $\sqrt{s}$ dependence of σ_{eff} extracted in different processes in different experiments, for an energy range between 63 GeV and 7 TeV.

criteria outlined in Section 2. This ratio was observed to be 11, with an associated systematic uncertainty of 5% due to background modelling [4]. The statistical uncertainty was negligible. The number of (exclusive) dijet events was found to be 28820 following the event selection criteria outlined in Section 2. The integrated luminosity was $\mathscr{L} = 184\ \mu\mathrm{b}^{-1}$, with a systematic uncertainty of 3.4% [19]. The trigger selection for dijet events is fully efficient ($\epsilon_{2\mathrm{j}} = 1$).

The lepton-jet overlap removal was only applied to jets in the $W + 2\mathrm{j}$ sample. A small correction was applied to account for any bias in the acceptance cancellation assumed in equation 5. The effect of $E_{\mathrm{T}}^{\mathrm{miss}}$ resolution on the acceptance cancellation was found to be negligible.

The final result is σ_{eff} (7 TeV) $= 11 \pm 1$ (stat) $^{+3}_{-2}$ (sys) mb. This is compared to results from previous experiments [20–24] as a function of centre-of-mass energy in Figure 5. The value of σ_{eff} obtained in this measurement is consistent with the Tevatron results assuming no energy dependence. However, given the quoted uncertainties on each measurement, a dependence on the centre-of-mass energy cannot be excluded.

References

[1] ATLAS Collaboration, "A measurement of hard double-partonic interactions in $W \to l\nu$ + 2 jet events", ATLAS-CONF-2011-160.

[2] B. Humpert, R. Odorico, "Multiparton scattering and QCD radiation as sources of four jet events", Phys. Lett. B **154** (1985) 211.

[3] ATLAS Collaboration, "The ATLAS Experiment at the CERN Large Hadron Collider", JINST **3** S08003 (2008).

[4] ATLAS Collaboration, "Measurement of the production cross section for W-bosons in association with jets in pp collisions using 33 $\mathrm{pb}^{-1}$of data at $\sqrt{s} = 7$ TeV with the ATLAS detector", Phys. Lett. B **698** (2011) 325-345.

[5] M. Cacciari, G. P. Salam, G. Soyez, "The anti-k_t jet clustering algorithm", JHEP **0408** (2008) 063.

[6] ATLAS Collaboration, "Measurement of inclusive jet and dijet cross sections in proton-proton collisions at 7 TeV centre-of-mass energy with the ATLAS detector", Eur. Phys. J. C **71** (2011) 1512.

[7] M. L. Mangano, M. Moretti, F. Piccinini, R. Pittau, A. D. Polosa, "ALPGEN, a generator for hard multiparton processes in hadronic collisions", JHEP **0307** (2003) 001.

[8] J. Alwall *et. al*, "Comparative study of various algorithms for the merging of parton showers and matrix elements in hadronic collisions", Eur. Phys. J. C **53** (2008) 473.

[9] G. Corcella *et. al*, "HERWIG 6: An Event generator for hadron emission reactions with interfering gluons (including supersymmetric processes)", JHEP **0101** (2001) 010.

[10] J. M. Butterworth, J. R. Forshaw, M. H. Seymour, "Multiparton interactions in photoproduction at HERA", Z. Phys. C **72** (1996) 637-646.

[11] ATLAS Collaboration, "First tuning of HERWIG/JIMMY to ATLAS data", ATL-PHYS-PUB-2010-014, 2010.

[12] T. Gleisberg, S. Hoeche, F. Krauss, M. Schonherr, S. Schumann, F. Siegert, J. Winter, "Event generation with SHERPA 1.1", JHEP **0902** (2009) 007.

[13] S. Catani, F. Krauss, R. Kuhn, B. R. Webber, "QCD matrix elements + parton showers", JHEP **0111** (2001) 063.

[14] T. Sjostrand, S. Mrenna, P. Z. Skands, "PYTHIA 6.4 Physics and Manual", JHEP **0605** (2006) 026.

[15] ATLAS Collaboration, "Charged particle multiplicities in pp interactions at $\sqrt{s} = 0.9$ at 7 TeV in a diffractive limited phase space measured with the ATLAS detector at the LHC and a new PYTHIA6 tune", Eur. Phys. J. C **70** (2010) 823.

[16] S. Frixione and B.R. Webber, "Matching NLO QCD computations and parton shower simulations", JHEP **0206** (2002) 029.

[17] ATLAS Collaboration, "The ATLAS simulation infrastructure", Eur. Phys. J. C **70** (2010) 823.

[18] S. Agostinelli et al. , "Geant4 - a simulation toolkit", Nucl. Inst. and Meth. A **506** (2003) 250.

[19] ATLAS Collaboration, "Updated Luminosity Determination in pp Collisions at $\sqrt{s} = 7$ TeV using the ATLAS Detector", ATLAS-CONF-2011-011.

[20] The AFS collaboration, "Double parton scattering in pp collisions at $\sqrt{s} = 63$ GeV", Z. Phys. C **34** (1987) 163.

[21] The UA2 Collaboration, "A Study of multi-jet events at the CERN $\bar{p}p$ collider and a search for double parton scattering", Phys. Lett. B **268** (1991) 145-154.

[22] The CDF Collaboration, "Study of four jet events and evidence for double parton interactions in $p\bar{p}$ collisions at $\sqrt{s} = 1.8$ TeV", Phys. Rev. D **47** (1993) 4857-4871.

[23] The CDF Collaboration, "Double parton scattering in $\bar{p}p$ collisions at $\sqrt{s} = 1.8$ TeV", Phys. Rev. D **56** (1997) 3811-3832.

[24] The D0 Collaboration, "Double parton interactions in photon+3 jet events in $\bar{p}p$ collisions $\sqrt{s} = 1.96$ TeV", Phys. Rev. D **81** (2010) 052012.